26

Nanoarchitectonic Design of Complex Materials Using Polymer Brushes as Structural and Functional Units

M. Lorena Cortez, Gisela Díaz, Waldemar A. Marmisollé, Juan M. Giussi, and Omar Azzaroni

Instituto de Investigaciones Fisicoquímicas Teóricas y Aplicadas (INIFTA), Universidad Nacional de La Plata, CONICET, La Plata, Argentina

26.1 Introduction

Many materials exhibit structures on multiple length scales—from nano to macro; indeed, in some materials, the structural and functional units themselves have structure.[1] This structural hierarchy can play a major part in determining their macroscopic properties and concomitantly guide the synthesis of new materials for specific applications. The science behind hierarchical and hybrid materials spans over multiple approaches. Let us think for a moment of how Nature deals with hierarchical and complex structures. For biomaterials involved in interfacial processes, common geometries include capillaries, dendrites, globules, hair-like, or fin-like attachments supported on larger substrates.[2] From many years now, significant efforts have been directed toward the fabrication of functional materials involving multiple length scales and functionalities in close resemblance to Nature. For example, porous fibrous structures can behave like lightweight solids. Depending on what is attached on their surfaces, these core structures can act as multishape-active composites. If nanobuilding blocks can be linked to other nanomaterials, then the resulting material could act synergistically to express enhanced functions from different counterparts. This concept integrating chemistry and form opens up the possibility of taking a functional material of any shape and size to afford new materials with concerted functions. From the synthetic viewpoint, nanotubes, nanofibers, thin films, and composite nanoparticles facilitate the required nanochemical control over different levels of space organization to obtain a variety of powerful materials in which a delicate interplay between

Polymer and Biopolymer Brushes: for Materials Science and Biotechnology, First Edition.
Edited by Omar Azzaroni and Igal Szleifer.

chemical identity, shape, and morphology dictates *function* and *utility*. It seems evident that the construction of hierarchical, hybrid, and complex architectures integrating a myriad of nanobuilding blocks and polymer brushes offers diverse chemical and physical properties that make these hybrid systems promising candidates for active components in multiple applications. However, it is important to consider that such complex nanoarchitectures require the tailored production and organization of complex matter displaying spatially addressed chemistry using different wet chemical processes and self-organization pathways. Therefore, to achieve this goal it is important to design strategies for the controlled preparation of multicomponent nanostructures on different settings. Research efforts on this matter are often referred to as "nanoarchitectonics," a term popularized by Ariga and co-workers.[3,4] Within this framework, the ample functional and structural versatility of polymer brushes make them "ideal" building blocks for "soft nanoarchitectonics." To this end, this work is entirely dedicated to bringing together the latest research on nanoarchitectonics applications of polymer brushes in multiple research areas. It is therefore hoped that the juxtaposition of different molecular and supramolecular approaches will contribute to the further evolution of this fascinating area of materials science.

26.2 Nanoparticles at Spherical Polymer Brushes: Hierarchical Nanoarchitectonic Construction of Complex Functional Materials

One of the first explorations combining spherical brushes and different nanomaterials was reported by Ballauff's group. These researchers extensively studied the construction of supramolecular hierarchical structures for catalysis through the integration of nanoparticles on the surface of spherical polyelectrolyte brushes.[5] Spherical polymer brushes represented by a solid core with dimensions in the 100-nm range onto which long polymer brushes are densely grafted were employed as platforms to grow metal nanoparticles. The strategy relied on the confinement/complexation of counterions that can be used to generate metal nanoparticles within the polyelectrolyte environment. One of attractive features of these hierarchical hybrid systems is their ease of manipulation that makes them excellent nanosystems for applications in catalysis,[6,7] including the use of platinum nanoparticles in heterogeneous hydrogenation reactions[8] and bimetallic Au–Pt nanoparticles for the oxidation of alcohols.[9]

Furthermore, the combination of different chemistries in different length scales also facilitated the preparation of composites of metal nanoparticles and TiO_2 immobilized in spherical polyelectrolyte brushes.[10] These composite hierarchical systems have been synthesized by reduction of the respective metal (Au, Pt, Pd) ions adsorbed on the surface of as-prepared TiO_2

nanoparticles that were previously confined into poly(styrene sodium sulfonate) brushes grafted on a polystyrene core. The nanoarchitectonic combination of nanomaterials in the form of very stable colloidal systems represents a most promising strategy to attain efficient heterogeneous photocatalysts. For instance, the photocatalytic activity of the hierarchical hybrid particles was two to five times higher than that of the pure TiO_2 particles. This finding was ascribed to the enhanced adsorption of the probe molecule at the metal NP@TiO_2@polyelectrolyte brush hierarchical interface.

A rather similar approach was proposed by Minko and co-workers[11] to fabricate hierarchically organized single-nanoparticle structures employing 200 nm silica cores modified with pH-responsive poly(2-vinylpyridine) brushes, into which 15 nm gold nanoparticles were synthesized. These authors showed that the pH-driven actuation (swelling and collapse) of the polymer brush resulted in the modulation of the interparticle distance and the concomitant shift in the maximum wavelength of the surface plasmon absorption peak. Such hierarchically assembled nanostructures present potential capabilities to be used as free-standing single-particle sensors in various miniaturized analytical systems. More recently, Puretskiy and Ionov have elegantly demonstrated the hierarchical construction of nanoparticle@microparticle systems employing polymer brushes as structural and functional units to synthesize raspberry-like particles.[12] The raspberry-like particles were prepared by immobilization of silica nanoparticles on the surface of silica microparticles previously modified with poly(glycidyl methacrylate) brushes. The raspberry-type microparticles were grafted with poly(pentafluorostyrene) chains and used as building blocks to create ultrahydrophobic surfaces.

26.3 Nanotube and Nanowire Forests Bearing Polymer Brushes

Seminal contribution from Jiang's lab described the modification of aligned carbon nanotubes (ACNT) films[13–16] with poly(*N*-isopropylacrylamide) (PNIPAM) brushes in order to confer thermoresponsive properties to the hierarchical architecture constituted of "soft" and "hard" counterparts.[17] Their results demonstrated that both the macroscopic and the microscopic properties of the modified ACNTs exhibit remarkable responsiveness, revealing that the polymer brush operates across the multiple length scales. On the macroscopic scale, the ACNT film showed temperature-dependent wettability, whereas on the microscopic scale atomic force microscopy imaging indicated that every single carbon nanotube constituting the hierarchical architecture is also thermoresponsive. In a similar vein and inspired by the nanofibrillar structures of gecko adhesives, Javey et al. explored the construction of chemical connectors using Ge/parylene nanowire forests modified with PNIPAM brushes.[18]

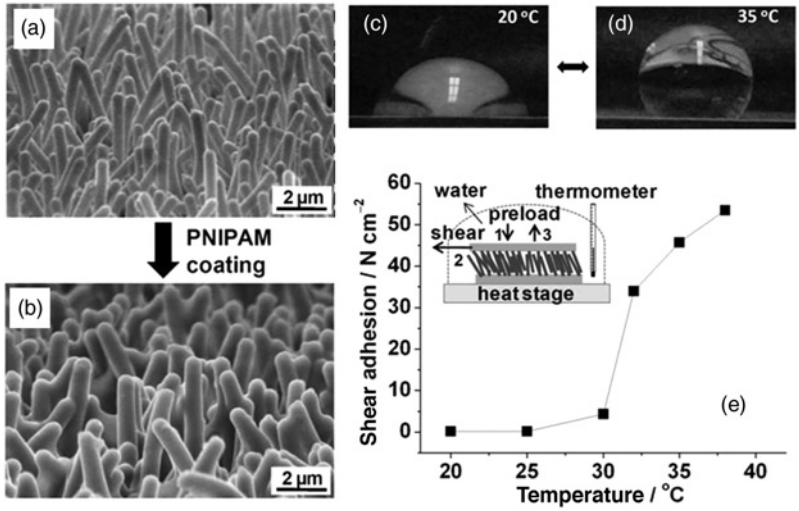

Figure 26.1 Scanning electron microscopy (SEM) micrographs of Ge/parylene nanowire (NW) forests (a) before and (b) after modification with PNIPAM brushes. Wetting properties of PNIPAM-modified NW forests at (c) 20°C and (d) 35°C. (e) Thermoresponsive shear adhesion strength of hybrid NW fasteners. *Source*: Ko et al. 2010.[18] Reproduced with permission of Wiley-VCH Verlag GmbH & Co. KGaA, Weinheim.

Several practical applications require the use of programmable fasteners that can change their adhesion properties on command. In this context, these authors designed hierarchical core/multishell hybrid forests with an outer shell of PNIPAM brushes capable of reversibly changing their wet adhesion strength in response to thermal changes of the environment. The distinctive thermoresponsive features of the PNIPAM brush outer layer in combination with the three-dimensional (3D) geometric configuration of the high aspect nanowire forest confers unique binding properties that arise from the tunable contribution of van der Waals interactions along with hydrophobic surface effects (Figure 26.1).

26.3.1 Polymer Brushes on Surfaces Displaying Microtopographical Hierarchical Arrays

It is a well-known fact that substrate geometry can amplify contact angle changes of responsive polymer brushes. In 2004, López and co-workers[19] demonstrated that changes in macroscopic surface hydrophobicity of polymer brushes can be quantitatively related to changes in surface nanostructure. These experiments were based on the modification of anodized nanoporous aluminum oxide with PNIPAM and conclusively showed that it is possible

to dynamically change the effective interfacial energy using surface-grafted stimuli-responsive polymers on roughened surfaces. In fact, this effect is much more significant when a substrate displaying microtopographical arrays is used. One of the first reports on this matter was contributed by Jiang et al.[20] showing the roughness-enhanced thermoresponsive wettability of PNIPAM brushes. Using a silicon substrate exhibiting a regular array of square silicon microconvexes that was modified with thin PNIPAM brushes (~45 nm), these authors demonstrated that despite of being a challenging subject in surface chemistry reversible switching between superhydrophilicity (contact angle (CA) ~ 0°) and superhydrophobicity (CA ~ 150°) is fully feasible. A similar concept was later used by Sun et al.[21] to create structured surfaces with solvent-responsive wettability. Well-aligned square micropillars modified with copolymer PNIPAM brushes bearing specially designed double amino acid units (Figure 26.2) displayed reversible wettability switching between superhydrophobicity and high hydrophilicity. The wettability switching was amplified due to the hierarchical nature of the substrate, a structured substrate composed of well-aligned square micropillars with a side length of about 10 μm and separation of about 12 μm, displaying nanofibrous structures on each pillar. According to the molecular design of the polymer brush, water treatment induces a dramatic

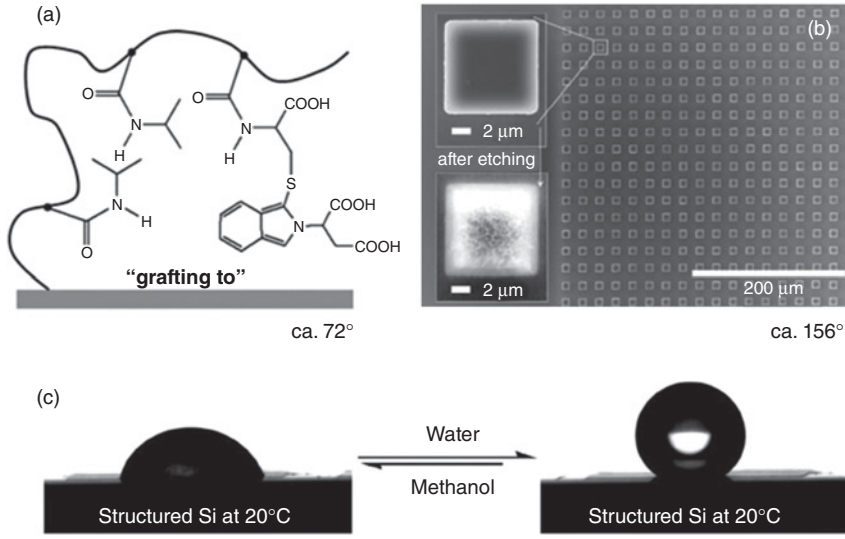

Figure 26.2 (a) Chemical structure of the copolymer brush containing double amino acid units. (b) SEM images of structured Si substrates. The insets correspond to single silicon pillars before (upper) and after chemical etching. Solvent responsive wetting properties of copolymer brush films containing double amino acid units: (a) after methanol treatment, (b) after water treatment. *Source*: Wang et al. 2009.[21] Reproduced with permission of Royal Society of Chemistry.

increase of hydrophobicity, whereas the hydrophilic state can be restored by the methanol–alkali treatment. This interesting phenomenon has been attributed to the strong but tunable hydrogen bonding, hydrophobic and electrostatic interactions interplay induced by the double amino acid units.

26.3.2 Environmentally Responsive Electrospun Nanofibers

If we look at forms of Nature, we observe that nanofibers are very attractive building blocks in the construction of hierarchically organized nanostructures. However, any successful design of multifunctional hierarchical materials using these elements demands a broad repertoire of nanofibers from a variety of materials to become available. During the past decade, electrospinning gained sound reputation as a versatile nanofiber fabrication technique enabling the preparation of superfine fibers with diameters ranging from 10 to 100 nm. In recent years, some groups started to explore the incorporation of polymer brushes on the surface of electrospun nanofibers with the aim of generating multilevel nanostructures on hierarchically organized composites. The size of the electrospun fibers can be in the nanoscale, and the fibers may possess different surface textures. The incorporation of polymer brushes to the fiber surface might lead to different modes of interaction with other materials compared with typical materials displaying no hierarchical organization. Brandl et al.[22] developed a rapid strategy to graft PNIPAM brushes from electrospun nanofibers using surface-initiated atom transfer radical polymerization (SI-ATRP) (Figure 26.3). The procedure simply involved electrospinning of an atom transfer radical polymerization (ATRP) macroinitiator and subsequent PNIPAM grafting using a "grafting-from" approach. The electrospun ATRP macroinitiator was based on a copolymer of methyl methacrylate (MMA) and 2-hydroxyethyl methacrylate, which was subsequently modified with

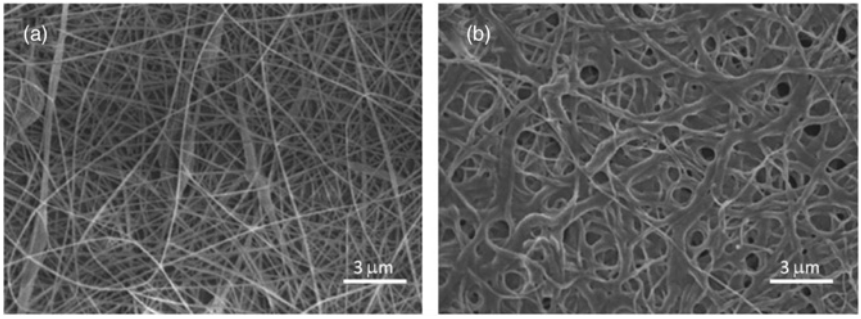

Figure 26.3 SEM micrographs of macroinitiator-modified nanofibers prior to (a) and after (b) surface-initiated polymerization of PNIPAM brushes. *Source*: Brandl et al. 2011.[22] Reproduced with permission of Wiley-VCH Verlag GmbH & Co. KGaA, Weinheim.

2-bromo-2-methylpropionyl bromide to introduce the ATRP initiators. The thermoresponsive properties of the poly(NIPAAm)-grafted films and fibers were corroborated by contact angle measurements. On the other hand, Kobayashi and co-workers[23] prepared electrospun nanofibers from a random copolymer of styrene and 4-vinylbenzyl 2-bromopropionate. Poly(styrene sulfonate) brushes were grown on the surface of the hydrophobic nanofibers, and the composite nanomaterials exhibited excellent water dispersibility owing to the hydrophilic brush layer.

26.4 Fabrication of Free-Standing "Soft" Micro- and Nanoobjects Using Polymer Brushes

Free-standing soft nanostructures are playing a more and more important role in the design of complex composite materials. Looking at Nature's complete technological design, we observe that many organisms are able to synthesize intricate free-standing architectures, for example, particles, capsules, tubes, wires, and so on, with meaningful nanostructures that cannot be reproduced using conventional synthetic strategies. Bottom-up construction of architectures as complex as those present in Nature is, of course, an impossible task. In view of this situation, several research groups considered particularly valuable to devise flexible methods to control structure and topology of polymer brushes to afford "soft" free-standing low-dimensional systems with different purposes. Pioneering work by Edmondson and Huck[24] demonstrated the preparation of quasi-two-dimensional (2D) polymer films by delaminating cross-linked poly(glycidyl methacrylate) brushes grafted onto gold substrates through controlled electrolysis (Figure 26.4). Free-standing, molecularly thin films based on cross-linked polymer brushes have the potential to act as tailorable scaffolds for ligands to promote polyvalent interactions at synthetic and biological surfaces or even as anisotropic elements in complex or liquid crystalline fluids. In very much the same way, the same group succeeded in controlling not only the formation of hybrid 2D polymer–metal composite microobjects[25] but also the folding of these 2D hybrid composites into 3D microstructures, like microcages or microcontainers.[26]

One of the first reports referring to the fabrication of polymeric nanospheres using polymer brushes was contributed by Walt and co-workers,[27] employing PBzMA-*co*-PEGDMA (poly(benzyl methacrylate-*co*-poly(ethylene glycol) dimethacrylate) brushes via SI-ATRP from SiO_2 particles to obtain hollow polymer particles after HF etching of the sacrificial silica cores. Nanocrystal templating has been also used by Möhwald and collaborators[28] to create capsules whose envelope was constituted of polymer brushes. In this approach, polymer capsules were prepared by SI-ATRP of 2-(dimethylamino)ethyl methacrylate brushes and its copolymers with

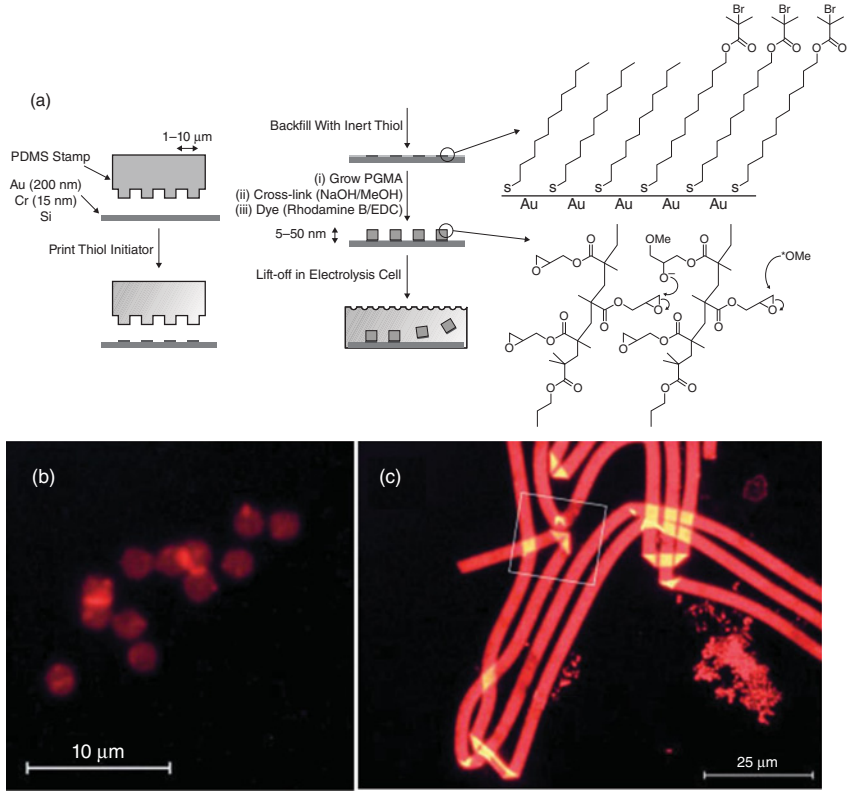

Figure 26.4 (a) Schematic describing the synthesis of quasi-2D polymer objects by micropatterning a gold surface using microcontact printing followed by growth of polymer brushes, cross-linking and electrochemical liftoff. (b) Fluorescence microscope image of 30 nm thick, 2 mm diameter polymer sheets, and (c) 3 mm wide lines obtained after electrochemical liftoff. *Source*: Edmondson and Huck 2004.[24] Reproduced with permission of Wiley-VCH Verlag GmbH & Co. KGaA, Weinheim.

2-(diethylamino)ethyl methacrylate and poly(ethylene glycol) methyl ether methacrylate from gold nanoparticles. Polymer brushes were cross-linked with 1,2-bis(2-iodoethoxy) ethane, and then KCN aqueous solutions were used to etch Au cores to yield the hollow capsules. These capsules showed swelling at low pH and shrinking at high pH as well as their ability to encapsulate and release rhodamine 6G. In line with these results, Kim et al. reported the "grafting-from" polymerization inside polyelectrolyte capsules and demonstrated that the interior of hollow "soft" particles can be locally modified with polymer brushes.[29] This clever strategy relies on the preparation of polyelectrolyte hollow capsules whose inner layer is coated with a water-soluble initiator, followed by polymerization of a desired monomer on the inner walls.

Monodisperse silica particles grafted with oxetane-bearing polymer brushes were also used to engineer and fabricate hollow spheres.[30] SI-ATRP of MMA with 3-ethyl-3-(methacryloyloxy)methyloxetane (EMO) from silica particles led to the formation core–shell systems exhibiting a block copolymer shell of the type poly(3-ethyl-3-(methacryloyloxy)methyloxetane)-block-poly(methyl methacrylate) (PEMO-*b*-PMMA). The inner PEMO block located between the PMMA outer shell and silica core was cross-linked by the cationic ring-opening reaction of the oxetane groups and subsequent removal of the inorganic core by HF etching gave polymeric hollow spheres (Figure 26.5). On the other hand, the synergistic combination of surface-initiated polymerization techniques and nanoporous membrane templating[31] has greatly facilitated the creation of complex and functional nanotubular structures. The approach takes advantage of both the new properties conferred by polymerizing diverse monomer units and the tight dimensional control offered by nanotemplating to enable new functionalities that arise from the highly anisotropic "one-dimensional" nanotube format. Li's group reported the synthesis of poly(*N*-isopropylacrylamide)-*co*-(*N*,*N*′-methylenebisacrylamide) (PNIPAM-*co*-MBAA) nanotubes with different composite ratios through SI-ATRP into nanoporous alumina templates.[32] These authors found that the dimension and shape of the nanotubes, especially the wall thickness, were highly dependent on the brush composition and, however, in all the cases, PNIPAM-*co*-MBAA nanotubes exhibited high flexibility and stability. A rather similar strategy was recently approached by Zou and co-workers to synthesize polymer nanograss and nanotubes by surface-initiated photopolymerization in cylindrical alumina nanopores.[33] In this case, they used pore-confined surface-initiated photopolymerization the mixture of glycidyl methacrylate (GMA) monomer and ethylene glycol dimethacrylate (EGDMA) as a cross-linker to obtain a variety of low-dimensional structures ranging from nanotubes to nanoneedles.

26.5 Solid-State Polymer Electrolytes Based on Polymer Brush–Modified Colloidal Crystals

Solid electrolytes represent a new class of solid-state ionic materials with potential applications in several technological areas as they exhibit an exceptionally high ionic conduction at room temperature. These properties make them ideal candidates for minimizing or even eliminating the shortcomings of liquid/aqueous electrolytes.[34] Very recently, Sato and co-workers[35] developed an interesting nanoarchitectonic approach for fabricating a leak- and vapor-free, nonflammable, and solid electrolytes with a highly ion-conductive network channel (Figure 26.6). The conceptual framework to develop such platforms was based on the 3D self-assembly of silica particles modified with ionic liquid-type polymer brushes. In this manner, the 3D scaffold facilitates

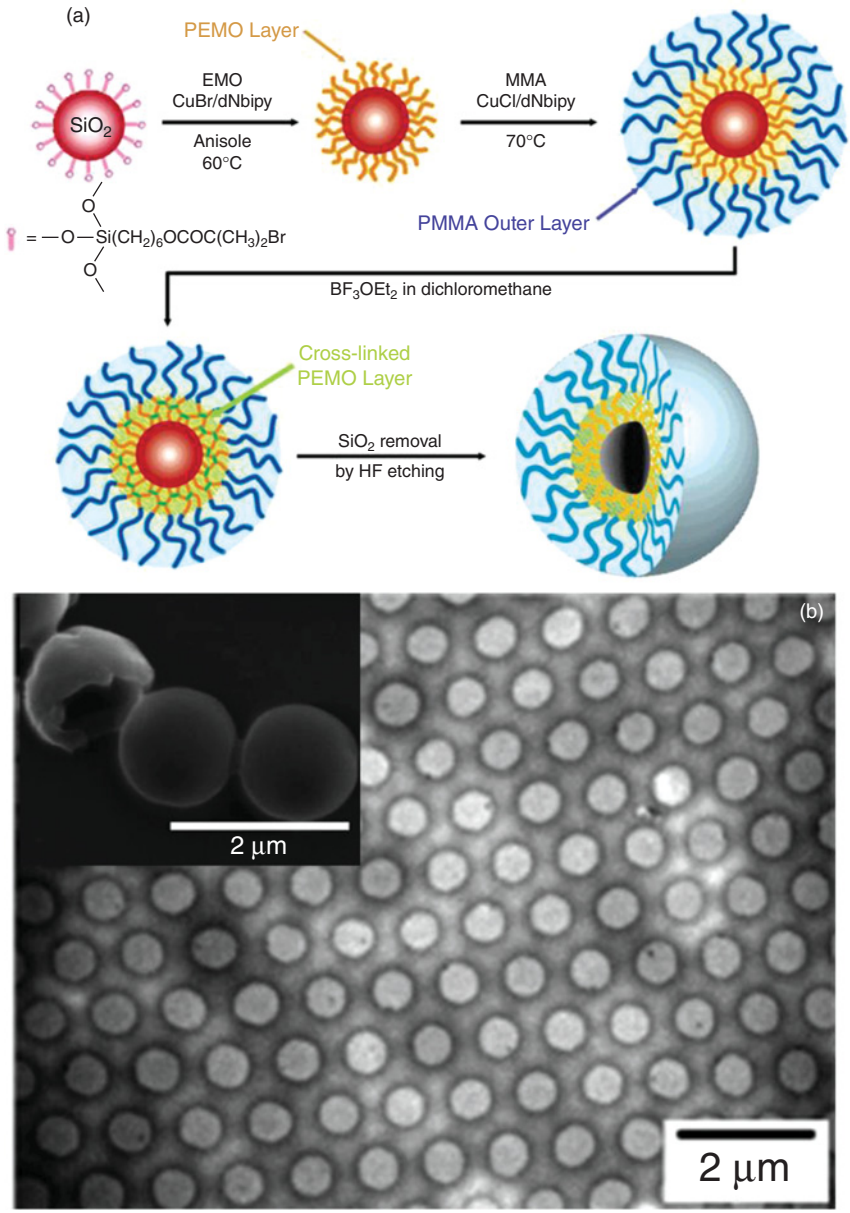

Figure 26.5 (a) Description of the synthetic steps involved in the fabrication of polymeric hollow spheres. (b) Transmission electron microscopic image of the hollow spheres. The inset shows a scanning electron micrograph of the polymeric hollow spheres. *Source*: Morinaga et al. 2007.[30] Reproduced with permission of American Chemical Society.

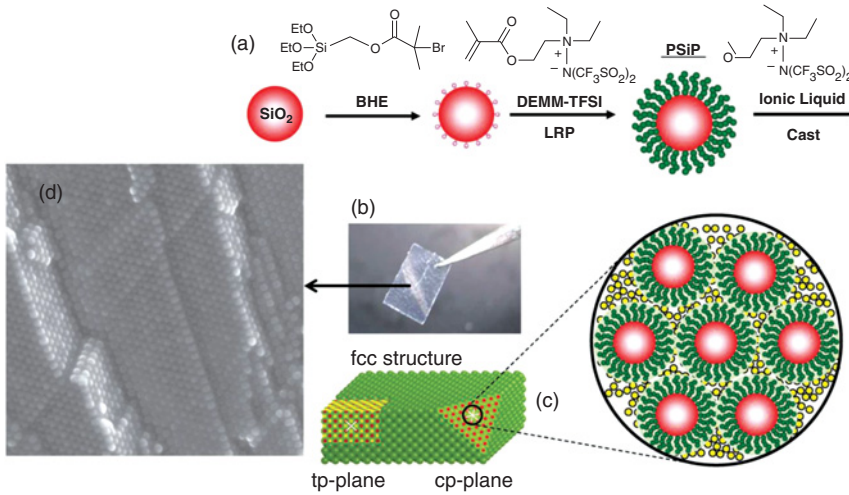

Figure 26.6 (a) Schematic representation of the preparation process of solid-state conductors via 3D self-assembly of silica particles modified with ionic liquid-type polymer brushes. (b) Photograph of produced hybrid solid film and (c) analyzed structure of hybrid array in solid state. (d) SEM image (15 000×) of a fractured hybrid solid film. *Source*: Sato et al. 2011.[35] Reproduced with permission of Wiley-VCH Verlag GmbH & Co. KGaA, Weinheim.

the formation of polymer brush domains continuously connected, forming network channels displaying enhanced ion conduction on the nanometer scale. As a proof of concept, a $Li_4Ti_5O_{12}$/hybrid solid electrolyte/$LiMn_2O_4$ unit cell was fabricated through the integration of the solid-state polymer electrolyte into a bipolar lithium-ion rechargeable battery and connected with a bipolar electrode of $Li_4Ti_5O_{12}$ (anode) and $LiMn_2O_4$ (cathode) layers. The Coulombic efficiency of this unit cell after 50 cycles was 98%, demonstrating that the nanoarchitectonic design of ion-conducting pathways using polymer brushes can improve the performance of lithium-ion rechargeable batteries.

26.6 Proton-Conducting Membranes with Enhanced Properties Using Polymer Brushes

Proton exchange membranes (PEMs) represent essential elements in energy conversion technologies.[36,37] In this context, Azzaroni and co-workers developed a nanoarchitectonic approach to create artificial proton-conducting channels based on the molecular design of well-oriented hydrophilic domains using polymer brushes (Figure 26.7).[38] Ordered 2D macroporous silicon membranes were modified with sulfonate-bearing polyelectrolyte brushes using pore-confined SI-ATRP in order to confer them proton-conducting properties.[39]

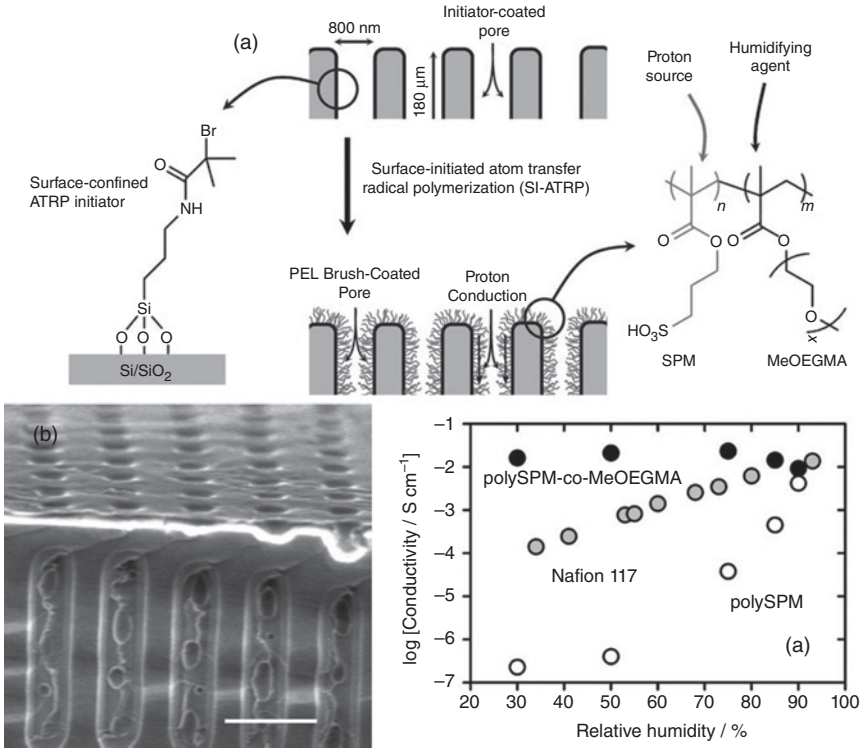

Figure 26.7 (a) Schematic representation of the pore-filling surface polymerization process used to create the proton-conducting channels. (b) Scanning electron micrograph corresponding to the macroporous silicon scaffold modified with the polymer brushes (scale bar: 3 μm). Conductivity versus relative humidity plots corresponding to the silicon membrane modified with polySPM-*co*-MeOEGMA brushes (black dots), the silicon membrane modified with polySPM brushes (white dots), and a Nafion 117 membrane (gray dots). *Source*: Yameen et al. 2009.[40] Reproduced with permission of Wiley-VCH Verlag GmbH & Co. KGaA, Weinheim.

The fabricated silicon-poly(sulfopropyl methacrylate) hybrid membranes exhibited proton conductivity as well as temperature- and humidity-dependent functional properties similar to that exhibited by typical Nafion membranes. These nanoarchitectured hybrid membranes displayed proton conductivities in the range of 10^{-2} S/cm. In another set of experiments, the same authors explored the integration of comonomers into the molecular design of the proton channel to improve the hydration of the polyelectrolyte bearing sulfonate groups. To this end, a small fraction of monomethoxy oligo-(ethylene glycol) methacrylate (MeOEGMA) was copolymerized with the sulfonate-bearing monomer. Poly(ethylene glycol) (PEG) derivatives exhibit excellent hydroscopic properties; hence, in the presence of PEGylated macromolecular architectures,

water molecules are able to form hydrogen bonds with the ethylene oxide units of the polymer chains. In this sense, proton conduction characterization revealed that the incorporation of a small fraction of MeOEGMA monomer units in the polyelectrolyte brush architecture promoted a five orders of magnitude increase in the proton conductivity measured at low relative humidities.[40] In addition, the nanoarchitectured platforms displayed high conductivity values ($\sim 10^{-2}$ S/cm[1]) regardless of the humidity, thus surpassing the performance of Nafion. These experiments illustrate the possibilities offered by "soft" nanoarchitectonics to fabricate tailorable proton-conducting membranes with highly optimized physical and chemical characteristics.

26.7 Hybrid Architectures Combining Mesoporous Materials and Responsive Polymer Brushes: Gated Molecular Transport Systems and Controlled Delivery Vehicles

The combination of mesoporous silica and polymer brushes has found an incredible resonance and a vast number of applications during the past decade, especially as drug delivery platforms. Due to its high surface area, large pore volume, and tunable pore size, mesoporous silica has been widely investigated as a potential candidate for drug delivery.[41] As a result of this situation, their surface modification with polymer brushes gained wide acceptance as a strategy to tailor the chemical properties of the porous materials. In this context, surface modification involving homogeneous derivatization of inner and outer surfaces using conventional "grafting-to" and "grafting-from" approaches has been extensively explored.

One of the first attempts to manipulate the transport properties of mesoporous materials using responsive polymer brushes was reported by López et al.[42] SI-ATRP was employed to graft PNIPAM brushes onto the inner and outer surfaces of mesoporous silica particles. These authors showed that below the lower critical solution temperature (LCST) swollen, hydrated PNIPAM brushes preclude the transport of solutes through the mesopores, whereas at higher temperatures (above LCST) brushes collapse on the pore walls, making the pores permeable to solutes. The same concept was then extended to the use of surface-initiated reversible addition fragmentation chain-transfer (SI-RAFT) to prepare PNIPAM-coated mesoporous silica nanospheres with controlled transport properties.[43] Later on, Oupicky and co-workers[44] demonstrated that selective modification of the outer surface of silica nanoparticles with PNIPAM brushes via a "grafting-to" approach was a plausible strategy to improve the thermo-triggered transport properties of the nanoarchitectured composite material. According to these authors, the selective modification of

the outer surface permitted the nanoconstruction of mesoporous delivery platforms exhibiting a low level of leakage upon switching the conformational state of the grafted chains. It should be noted that this mode of operation is opposite to that typically observed in mesoporous systems in which the PNIPAM is grown from the surface of the porous silica, that is diffusion occurs when the brush is swollen and retarded when it is collapsed.

On the other hand, Martínez-Máñez and co-workers reported for the first time the use of brush-like architectures to control the gating properties of mesoporous material by ion and pH modulation.[45] This by grafting of polyamines on the external surface of mesoporous silica scaffolds, the opening and closure of the mesopores was controlled via either hydrogen-bonding interactions between deprotonated amines (open pores) or Coulombic repulsions between protonated amino groups (closed pores). Under acidic conditions, the amines are fully protonated, the gate is closed, and access to the inner pores is precluded. In contrast, under neutral conditions the amines are deprotonated, the gate is open, and probe molecules can enter the pores. Concomitantly, an anion-controlled effect was also observed. In the neutral pH region, the gate is only open in the presence of small anions such as Cl^-, whereas bulky anions such as adenosine 5′-triphosphate (ATP) close the gate through formation of strong complexes with the amines at the pore entrance.

More recently, several groups explored similar strategies to synthesize pH-modulable brush-coated mesoporous particles. SI-ATRP has been employed to prepare poly(2-(diethylamino)ethyl methacrylate)-coated mesoporous silica nanoparticles resulting in hybrid nanoparticles with a pH-sensitive polymer shell and mesoporous core.[46] poly(2-(diethylamino)ethyl methacrylate) (PDEAEMA) brushes act as good "gatekeepers" to control access to the pores via a pH-dependent open-close mechanism, which was confirmed by the well-controlled release of rhodamine B from the mesopores by adjusting the solution pH. Poly(acrylic acid) brushes grafted onto the pore outlets of mesoporous silica via SI-RAFT polymerization were also employed to create "smart" nanogates sensitive to pH variations.[47] Feng and co-workers used a "grafting-to" strategy to anchor poly(vinylpyridine) (PVP) brushes onto mesoporous silica surfaces, resulting in a proton-gated macromolecular barrier suitable for drug delivery purposes.[48] Under neutral or slightly alkaline conditions, PVP brushes are collapsed on the pore entrance, thus blocking the passage of species trapped in the interior of the mesoporous particle. Upon lowering the pH conditions, the protonated brushes become swollen and permeable to the trapped molecule. On the other hand, the use of cross-linked polymer brushes as "gatekeepers" on the surface of mesoporous silica-based nanomaterials enables the gating operation in the presence of redox stimuli.[49] Poly(*N*-acryloxysuccinimide) brushes were grafted at the pore entrance of mesoporous particles. After loading the dye molecules into the particles, the openings are blocked by the addition of cystamine, a disulfide-based

bifunctional primary amine, which allows polymer chains to be cross-linked through the reaction between cystamine and *N*-oxysuccimide groups along the polymer chain. The cross-linked macromolecular barrier formed around the pore opening can be reopened by cleaving the disulfide bond of cystamine in the presence of dithiothreitol, a disulfide reducing agent. In this setting, the gating mechanism relies on redox reactions in which the cross-linked polymer brush works as an off–on switch in response to redox signals.

Modification of mesoporous silica thin films with polyelectrolyte brushes has also been explored as a strategy to manipulate the permselective properties of the membrane-like interfaces.[50] In this nanoarchitectured films, the solvent and the mobile ionic species are confined into the nanodomains of the polyelectrolyte brushes hosted in the mesoporous matrix. Depending on the nature of the interaction between the polyelectrolyte brushes and the ionic species (attractive or repulsive), diffusion through the pore can be feasible or not. In a similar vein, the integration of poly[2-(methacryloyloxy) ethyl phosphate] brushes into and onto mesoporous silica thin films permitted the creation of mesostructured interfaces with reversible gate-like transport properties that can be controlled not only by protons but also by calcium ions.[51] The ion-gate response/operation was based on the protonation and/or chelation of phosphate monomer units in which the polyelectrolyte brush works as an off–on switch in response to the presence of protons or Ca^{2+} ions.

On the other hand, the creation of photoactive hybrid polymer brush–inorganic assemblies displaying light-activated gating and permselective transport of ionic species was described by Brunsen et al.[52] The combination of "caged" poly2-[(4,5-dimethoxy-2-nitrobenzoxy) carbonyl] aminoethyl methacrylate (PNVOCAMA) brushes and mesoporous oxide thin films gave rise to the nanoarchitectonic design of photoactive interfaces. Owing to the hydrophobic and bulky nature of the monomers that precludes their free diffusion into the hydrophilic inner environment of the nanoporous framework, surface-initiated polymerization of NVOCAMA monomers on initiator-functionalized mesoporous films resulted in the selective growth of the photolabile brush atop the mesoporous film.

Selective modification of the "outer" layer of the hybrid-mesostructured film proved decisive to control the gating properties. The hydrophobic nature of the outer PNVOCAMA layer precludes hydrated ions from entering into the mesopores and diffusing across the interfacial nanoarchitecture. Then, light exposure resulted in the cleavage of the chromophore from the polymer layer generating poly(2-aminoethyl methacrylate) brushes that upon protonation under acidic solutions confer permselective properties to the nanoarchitectured mesoporous film.

Another interesting example of "soft" nanoarchitectonics is the synergistic integration of polymer brushes and mesoporous materials to attain hybrid materials with unusual properties. In this sense, Calvo et al.[53] have

demonstrated that the interplay between the intrinsic acid–base properties of silica mesoporous frameworks and the pH-responsive properties of weak zwitterionic brushes can gave rise to new proton-gated cation-selective membranes with properties observed neither in mesoporous films nor in brushes. Mesoporous silica thin films modified with zwitterionic poly(methacryloyl-L-lysine) brushes act as gateable ionic filters modulating the passage of cations while inhibiting the passage of anions over a wide pH range. This behavior closely resembles the gating properties of biological acid-sensing ion channels. According to these authors, a "bipolar" Donnan exclusion phenomenon is responsible for building up, in a reversible manner, a chemically actuated ionic barrier under acidic conditions. The bipolar environment arises from the synergistic coexistence of negative charges due to the silanolate groups on the silica pore walls and positive charges due to the protonated methacryloyl-L-lysine monomer units on the brush layer.

Results discussed in this section reveals that the combination of polymer brushes and mesoporous materials offers a wide range of opportunities for materials *nanoarchitectonics*[54–56] provided that these hybrid systems can exhibit functional domains ordered in space. In fact, the integration of polymer brushes into mesoporous scaffolds bring about the possibility to create phase-separated regions (functional domains) within the pores that can behave as "gatekeepers" of nanoscale size.

26.8 Ensembles of Metal Nanoparticles Modified with Polymer Brushes

Nowadays, it is widely accepted that the control of order and periodicity of 3D arrangements of inorganic nanoparticles can be exploited at a whole new level to design a broad variety of new materials and devices.[57] Ensembles of nanoparticles can display new electronic, magnetic, and optical properties as a result of interactions between the excitons, magnetic moments, or surface plasmons of individual nanoobjects.[58] However, before reaching this level of synthetic control and design, it is first necessary to finely tune the interactions between neighboring nanoparticles as well as between the nanoparticles and their surrounding environment. In this regard, polymer brushes grafted to the surface of the colloidal particles[59] can play a decisive role in attaining highly tunable conditions leading to the stable formation of ensembles of nanoparticles in a controllable manner.

Seminal work of Fukuda's group described early attempts to build up ordered arrays of gold nanoparticles coated with high-density PMMA brushes through the implementation of the Langmuir–Blodgett technique (Figure 26.8).[60] Owing to the high surface density and the controlled chain length, grafted PMMA chains at the air–water interface exert interparticle interactions of an

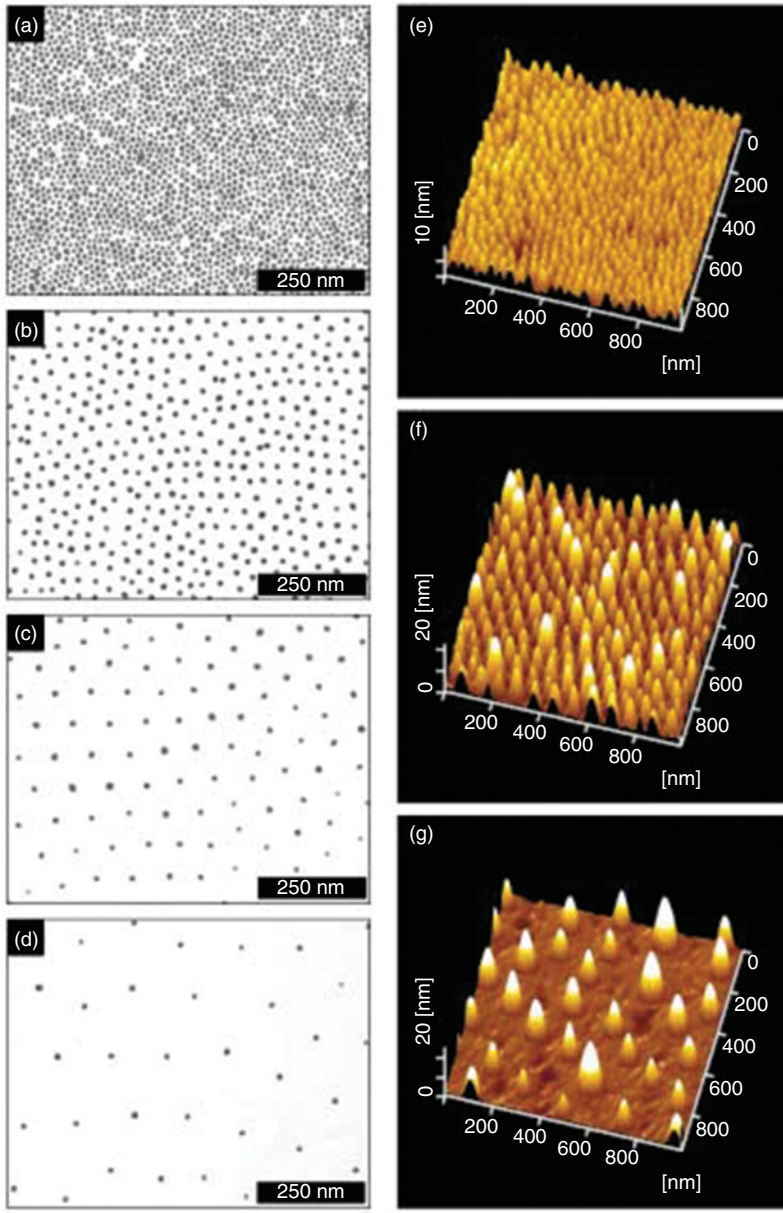

Figure 26.8 TEM images of the transferred nanoparticle films corresponding to (a) initiator-coated Au nanoparticles and (b–d) Au-nanoparticle–PMMA hybrids: Mn of the PMMA graft (b) 1,2000, (c) 28,000, and (d) 62,000. (e–g) AFM images of the transferred films of Au-nanoparticle–PMMA hybrids: Mn of the PMMA graft (e) 12,000, (f) 28,000, and (g) 62,000. *Source*: Ohno et al. 2003.[60] Reproduced with permission of Wiley-VCH Verlag GmbH & Co. KGaA, Weinheim.

extremely long range and, consequently, the Au-nanoparticle–PMMA hybrids form a 2D array with a high degree of structural order that translates into an exceptional controllability of the interparticle distance. 2D self-organization was also demonstrated for polystyrene-capped gold nanoparticles.[61] The polystyrene brush-modified nanoparticles self-organize into hexagonally ordered monolayers when cast onto solid substrates from chloroform solutions, and the distance between the gold cores in the dried monolayer can be easily controlled by the molecular weight of the grafted polystyrene chains.

Controlling the spatial distribution of the macromolecular units located at the nanoparticle surface offers a broad range of alternatives to nanoparticle systems with controlled anisotropy which can be used in a number of applications. Wang et al.[62] synthesized Janus-type gold nanoparticles using bicompartment polymer brushes (PMMA and poly(ethylene oxide) (PEO)) leading to the formation of hybrid nanobuilding blocks with the following stoichiometry: PEO_{114}-Au_6-$PMMA_{208}$. Mixed brush-coated nanoparticles (NPs) are soluble in good solvents for PMMA and PEO, such as acetone, chloroform, tetrahydrofuran, and dimethylformamide, but they have a well-defined tendency to form particle clusters and wormlike aggregates in dioxane and dioxane/acetone mixed solvents. This phenomenon was attributed to PEO-mediated particle assembly. Note, however, that Janus-type configurations are not the only scenarios allowing two different types of chemistry to occur on the same particle. By exploiting the amphiphilic properties of gold nanoparticles coated with mixed polymer brushes of PEG and PMMA, the assembly of plasmonic dimers was recently demonstrated.[63] Formation of dimeric nanoparticle assemblies is of considerable interest for applications requiring strong near-field coupling of surface plasmon resonances. In this case, Duan and co-workers showed that Au NPs functionalized with amphiphilic brush-type coatings preferentially form dimers in water due to the collapse and aggregation of hydrophobic grafts and reorganization of hydrophilic grafts (Figure 26.9). As a result, the interparticle plasmonic coupling can be reversibly controlled by modulating the assembly/disassembly of the amphiphilic nanoparticles in different environmental conditions. Using a similar approach, the same group created responsive plasmonic assemblies at oil–water interfaces in which the plasmon coupling of gold nanoparticle and nanorod ensembles was reversibly modulated by conformational changes in the polymeric coating.[64] Nanocrystals modified with mixed PEG and PMMA brushes displayed collective plasmonic properties that could be tailored by changing solvent quality, whereas those modified with mixed PEG and poly(2-(diethylamino)ethyl methacrylate) brushes display pH-dependent assembling properties.

Edwards et al.[65] demonstrated that increasing the solution temperature of poly(poly(ethylene glycol) methyl ether monomethacrylate) (PPEGMA)-coated gold nanoparticles above the LCST of the polymer triggers reversible transport of the nanoparticles across an oil/water interface. Boyer et al.[66] have

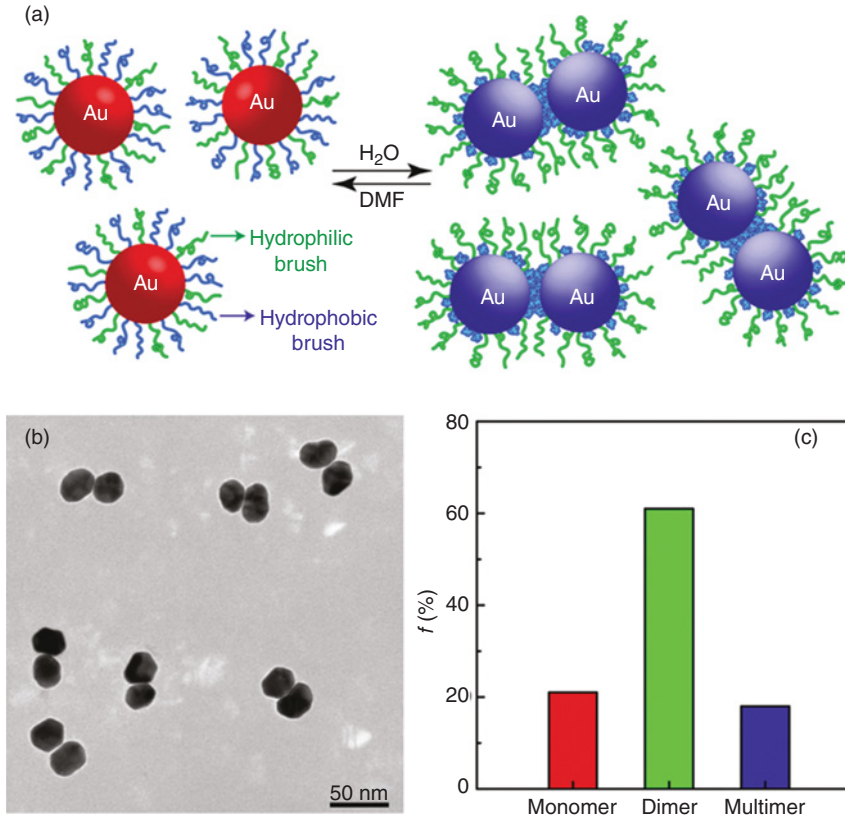

Figure 26.9 (a) Schematic representation of the solvent-induced self-assembly of amphiphilic gold nanocrystals modified with mixed PEG and PMMA polymer brushes. (b) TEM image of the self-assembled dimmers. (c) Statistical fractions of monomer, dimer, and multimeric structures. *Source*: Cheng et al. 2011.[63] Reproduced with permission of American Chemical Society.

coated 20 nm gold nanoparticles with copoly(oligo ethylene glycol)acrylates with LCSTs between 15 and 92°C and demonstrated that the thermoresponsive properties of the polymer–gold hybrids can be tuned by adjusting the composition of the polymer coating.

In a similar vein, Gehan et al.[67] also described the combination of solid-supported lithographically fabricated gold NPs and thermoresponsive PNIPAM brushes to generate calibrated and dynamically controlled hybrid gold/polymer architectures for real-time nanosensing based on the phase transition of the polymer layer. Rezende and co-workers[68] further explored the formation of stable Langmuir monolayers of gold nanoparticles grafted with thermosensitive PNIPAM brushes. At low surface concentration, the gold

nanoparticles are attached to the surface by PNIPAM chains adsorbed in a pancake conformation yielding a thin and compact layer. Upon isothermal compression, the chains are reorganized to form brush-type structures immersed in the bulk phase. Upon increasing the working temperature PNIPAM chains collapse with the corresponding decrease in the interparticle distance. The reversibility of the macromolecular reorganization at the air–liquid interface was used as a reversible thermoswitch to modulate the interparticle distance and the dielectric environment of gold nanoparticle monolayers.

A recent work by Klok's group[69] investigated the thermoresponsive properties of PPEGMA-coated gold nanoparticles with gold core diameters in the 5–47 nm range. According to their experimental evidence, these systems not only display size-dependent LCST transitions but also show cooperative thermosensitive behavior. This indicates that a PPEGMA-coated particle with a relatively high LCST can cooperatively assemble with another PPEGMA-coated particle with a lower LCST. This interesting cooperative aggregation phenomenon was utilized to manipulate the assembly of nanoparticles onto surfaces through the capture and binding of PPEGMA-coated nanoparticles on substrates modified with complementary thermoresponsive PPEGMA brushes. *These results open a new perspective* in the practical applications on thermoresponsive coatings provided that these findings could be exploited for enzyme recovery, protein purification, or even the thermotriggered creation of structured nanoparticle thin films.

Very recently, Duan and co-workers[70] reported on an interesting approach leading to a new class of turn-on surface enhanced Raman scattering (SERS) sensors for the sensitive and selective detection of cadmium ion (Cd^{2+}) by taking advantage of the interparticle plasmonic coupling generated in the process of Cd^{2+}-selective nanoparticle self-aggregation. Their approach is based on the use of gold nanoparticles modified with a Raman-active dye and a polymer brush layer displaying Cd^{2+}-chelating properties. Addition of Cd^{2+} to the test solution promotes interparticle self-aggregation and immediately turns on the SERS fingerprint signal with up to 90-fold of signal enhancement. Control experiments with various metal ions confirmed that the platform is specific to Cd^{2+} ions, and, in contrast to other nanoparticle-based colorimetric assays, the method proved capable of detecting Cd^{2+} in heavily colored samples. This strategy clearly reveals the possibility for developing hybrid materials with integrated and collective functionalities.

26.9 Conclusions

Nanoarchitectonics is aimed at arranging nanoscale structural units into a configuration that creates a novel functionality through mutual interactions among those units. In this chapter, we have shown that polymer brushes can be used

as structural and functional units to create novel nanoarchitectures displaying new functionalities arising from the delicate interplay of their nanoscale building blocks.

Examples described in this chapter clearly reveal that chemists and material scientists have learnt many ways to combine concepts and tools from self-assembly and supramolecular chemistry to construct complex, hybrid, and hierarchical materials. However, it seems evident that a higher degree of structural sophistication and functionality probably cannot yet be obtained by sole reliance on the combination of self-assembly and supramolecular interactions. Controlled incorporation of polymer brushes into the nanoarchitectured systems can yield unique nanomaterials that have neither inorganic nor polymeric analogues. While most inorganic nanoarchitectures constitute a topologically well-defined but rigid structure, polymer brushes exhibit a flexible nature. In this context, the new horizons provided by "soft" nanoarchitectonics appear very wide and the future offers the prospect of many developments as chemists and material scientists show an increased mastery in construction of nanoarchitectures combining structural features and functional properties of inorganic materials and polymer brushes.

The evolution of nanoarchitectonics at the beginning of this century was accompanied by applications of these developments in different technological areas. Yet, there is a need to keep exploring new avenues to attain hybrid, complex, and hierarchical nanoarchitectures exhibiting strictly controlled structure, topology, and function. We believe that this is the cornerstone to convert molecular functions into macroscopic properties expressed at the level of the architectured assemblies, thus leading to the nanoarchitectonic design and production of addressable molecular materials.

Acknowledgments

The authors acknowledge financial support from ANPCyT (PICT 2010-2554, PICT-2013-0905), Fundación Petruzza, Consejo Nacional de Investigaciones Científicas y Técnicas (CONICET) (PIP 0370) and the Austrian Institute of Technology GmbH (AIT–CONICET Partner Lab: *"Exploratory Research for Advanced Technologies in Supramolecular Materials Science"* – Exp. 4947/11, Res. No. 3911, 28-12-2011). J.M.G., M.L.C., W.A.M., and O.A. are CONICET fellows.

References

1 Pagliaro, M.; Ciriminna, R.; Palmisano, G. *Chem. Rec.* **2010**, *10* (1), 17–28.

2 Ante, A.; Budimir, M. In *Engineering the Future*; Dudas, L.; INTECH: Vienna, 2010; pp. 26–46.

3 Aono, M.; Ariga, K. *Adv. Mater.* **2016**, *28* (6), 989–992.
4 Ariga, K.; Li, J.; Fei, J.; Ji, Q.; Hill, J. P. *Adv. Mater.* **2016**, *28* (6), 1251–1286.
5 Lu, Y.; Wittemann, A.; Ballauff, M. *Macromol. Rapid Commun.* **2009**, *30* (9–10), 806–815.
6 Wunder, S.; Polzer, F.; Lu, Y.; Mei, Y.; Ballauff, M. *J. Phys. Chem. C* **2010**, *114* (19), 8814–8820.
7 Mei, Y.; Lu, Y.; Polzer, F.; Ballauff, M.; Drechsler, M. *Chem. Mater.* **2007**, *19* (5), 1062–1069.
8 Sharma, G.; Mei, Y.; Lu, Y.; Ballauff, M.; Irrgang, T.; Proch, S.; Kempe, R. *J. Catal.* **2007**, *246* (1), 10–14.
9 Schrinner, M.; Proch, S.; Mei, Y.; Kempe, R.; Miyajima, N.; Ballauff, M. *Adv. Mater.* **2008**, *20* (10), 1928–1933.
10 Lu, Y.; Lunkenbein, T.; Preussner, J.; Proch, S.; Breu, J.; Kempe, R.; Ballauff, M. *Langmuir* **2010**, *26* (6), 4176–4183.
11 Lupitskyy, R.; Motornov, M.; Minko, S. *Langmuir* **2008**, *24* (16), 8976–8980.
12 Puretskiy, N.; Ionov, L. *Langmuir* **2011**, *27* (6), 3006–3011.
13 Ren, Z. F.; Huang, Z. P.; Xu, J. W.; Wang, J. H.; Bush, P.; Siegal, M. P.; Prevencio, P. N. *Science* **1998**, *282* (5391), 1105–1107.
14 Wei, B. Q.; Vajtai, R.; Jung, Y.; Ward, J.; Zhang, R.; Ramanath, G.; Ajayan, P. M. *Nature* **2002**, *416* (6880), 495–496.
15 Liu, H.; Li, S.; Zhai, J.; Li, H.; Zheng, Q.; Jiang, L.; Zhu, D. *Angew. Chem., Int. Ed.* **2004**, *43* (9), 1146–1149.
16 Xia, F.; Zhu, Y.; Feng, L.; Jiang, L. *Soft Matter* **2009**, *5* (2), 275–281.
17 Sun, T.; Liu, H.; Song, W.; Wang, X.; Jiang, L.; Li, L.; Zhu, D. *Angew. Chem., Int. Ed.* **2004**, *43* (35), 4663–4666.
18 Ko, H.; Zhang, Z.; Chueh, Y.-L.; Saiz, E.; Javey, A. *Angew. Chem., Int. Ed.* **2010**, *49* (3), 616–619.
19 Fu, Q.; Rama Rao, G. V.; Basame, S. B.; Keller, D. J.; Artyushkova, K.; Fulghum, J. E.; López, G. P. *J. Am. Chem. Soc.* **2004**, *126* (29), 8904–8905.
20 Sun, T.; Wang, G.; Feng, L.; Liu, B.; Ma, Y.; Jiang, L.; Zhu, D. *Angew. Chem.* **2004**, *116* (3), 361–364.
21 Wang, X.; Qing, G.; Jiang, L.; Fuchs, H.; Sun, T. *Chem. Commun.* **2009**, No. *19*, 2658.
22 Brandl, C.; Greiner, A.; Agarwal, S. *Macromol. Mater. Eng.* **2011**, *296* (9), 858–864.
23 Yoshikawa, C.; Zhang, K.; Zawadzak, E.; Kobayashi, H. *Sci. Technol. Adv. Mater.* **2011**, *12* (1), 15003.
24 Edmondson, S.; Huck, W. T. S. *Adv. Mater.* **2004**, *16* (15), 1327–1331.
25 Comrie, J. E.; Huck, W. T. S. *Langmuir* **2007**, *23* (3), 1569–1576.
26 Kelby, T. S.; Wang, M.; Huck, W. T. S. *Adv. Funct. Mater.* **2011**, *21* (4), 652–657.
27 Mandal, T. K.; Fleming, M. S.; Walt, D. R. *Chem. Mater.* **2000**, *12* (11), 3481–3487.

28 Duan, H.; Kuang, M.; Zhang, G.; Wang, D.; Kurth, D. G.; Möhwald, H. *Langmuir* **2005**, *21* (24), 11495–11499.

29 Choi, W. S.; Park, J.-H.; Koo, H. Y.; Kim, J.-Y.; Cho, B. K.; Kim, D.-Y. *Angew. Chem., Int. Ed.* **2005**, *44* (7), 1096–1101.

30 Morinaga, T.; Ohkura, M.; Ohno, K.; Tsujii, Y.; Fukuda, T. *Macromolecules* **2007**, *40* (4), 1159–1164.

31 Azzaroni, O.; Lau, K. H. A. *Soft Matter* **2011**, *7* (19), 8709–8724.

32 Cui, Y.; Tao, C.; Tian, Y.; He, Q.; Li, J. *Langmuir* **2006**, *22* (19), 8205–8208.

33 Zou, C.; Luo, Z.; Le, D. H.; Dessources, K.; Robles, A.; Chen, G. *J. Mater. Chem.* **2011**, *21* (38), 14543.

34 Agrawal, R. C.; Pandey, G. P. *J. Phys. D. Appl. Phys.* **2008**, *41* (22), 223001.

35 Sato, T.; Morinaga, T.; Marukane, S.; Narutomi, T.; Igarashi, T.; Kawano, Y.; Ohno, K.; Fukuda, T.; Tsujii, Y. *Adv. Mater.* **2011**, *23* (42), 4868–4872.

36 Srinivasan, S. In *Fuel Cells: From Fundamentals to Applications*; Springer: Berlin, 2006; pp. 575–605.

37 Bussian, D. A.; O'Dea, J. R.; Metiu, H.; Buratto, S. K. *Nano Lett.* **2007**, *7* (2), 227–232.

38 Yameen, B.; Kaltbeitzel, A.; Langner, A.; Duran, H.; Müller, F.; Gösele, U.; Azzaroni, O.; Knoll, W. *J. Am. Chem. Soc.* **2008**, *130* (39), 13140–13144.

39 Yameen, B.; Kaltbeitzel, A.; Glasser, G.; Langner, A.; Muüller, F.; Goüsele, U.; Knoll, W.; Azzaroni, O. *ACS Appl. Mater. Interfaces* **2010**, *2* (1), 279–287.

40 Yameen, B.; Kaltbeitzel, A.; Langer, A.; Müller, F.; Gösele, U.; Knoll, W.; Azzaroni, O. *Angew. Chem., Int. Ed.* **2009**, *48* (17), 3124–3128.

41 Vallet-Regí, M.; Balas, F.; Arcos, D. *Angew. Chem., Int. Ed.* **2007**, *46* (40), 7548–7558.

42 Fu, Q.; Rao, G. V. R.; Ista, L. K.; Wu, Y.; Andrzejewski, B. P.; Sklar, L. A.; Ward, T. L.; López, G. P. *Adv. Mater.* **2003**, *15* (15), 1262–1266.

43 Chung, P.-W.; Kumar, R.; Pruski, M.; Lin, V. S.-Y. *Adv. Funct. Mater.* **2008**, *18* (9), 1390–1398.

44 You, Y.-Z.; Kalebaila, K. K.; Brock, S. L.; Oupicky D. *Chem. Mater.* **2008**, *20* (10), 3354–3359.

45 Casasús, R.; Marcos, M. D.; Martínez-Máñez, R.; Ros-Lis, J. V.; Soto, J.; Villaescusa, L. A.; Amorós, P.; Beltrán, D.; Guillem, C.; Latorre, J. *J. Am. Chem. Soc.* **2004**, *126* (28), 8612–8613.

46 Sun, J.-T.; Hong, C.-Y.; Pan, C.-Y. *J. Phys. Chem. C* **2010**, *114* (29), 12481–12486.

47 Hong, C.-Y.; Li, X.; Pan, C.-Y. *J. Mater. Chem.* **2009**, *19* (29), 5155.

48 Liu, R.; Liao, P.; Liu, J.; Feng, P. *Langmuir* **2011**, *27* (6), 3095–3099.

49 Liu, R.; Zhao, X.; Wu, T.; Feng, P. *J. Am. Chem. Soc.* **2008**, *130* (44), 14418–14419.

50 Calvo, A.; Yameen, B.; Williams, F. J.; Azzaroni, O.; Soler-Illia, G. J. A. A. *Chem. Commun.* **2009**, *18*, 2553–2555.

51 Brunsen, A.; Díaz, C.; Pietrasanta, L. I.; Yameen, B.; Ceolín, M.; Soler-Illia, G. J. A. A.; Azzaroni, O. *Langmuir* **2012**, *28* (7), 3583–3592.

52 Brunsen, A.; Cui, J.; Ceolín, M.; Campo, A. del; Soler-Illia, G. J. A. A.; Azzaroni, O. *Chem. Commun.* **2012**, *48* (10), 1422–1424.

53 Calvo, A.; Yameen, B.; Williams, F. J.; Soler-Illia, G. J. A. A.; Azzaroni, O. *J. Am. Chem. Soc.* **2009**, *131* (31), 10866–10868.

54 Ariga, K.; Vinu, A.; Yamauchi, Y.; Ji, Q.; Hill, J. P. *Bull. Chem. Soc. Jpn.* **2012**, *85* (1), 1–32.

55 Ariga, K.; Hill, J. P.; Lee, M. V; Vinu, A.; Charvet, R.; Acharya, S. *Sci. Technol. Adv. Mater.* **2008**, *9* (1), 14109.

56 Soler-Illia, G. J. A. A.; Azzaroni, O. *Chem. Soc. Rev.* **2011**, *40* (2), 1107–1150.

57 Brust, M. *Nat. Mater.* **2005**, *4* (5), 364–365.

58 Nie, Z.; Petukhova, A.; Kumacheva, E. *Nat. Nanotechnol.* **2010**, *5* (1), 15–25.

59 Dong, H.; Zhu, M.; Yoon, J. A.; Gao, H.; Jin, R.; Matyjaszewski, K. *J. Am. Chem. Soc.* **2008**, *130* (39), 12852–12853.

60 Ohno, K.; Koh, K.; Tsujii, Y.; Fukuda, T. *Angew. Chem., Int. Ed.* **2003**, *42* (24), 2751–2754.

61 Yockell-Lelièvre, H.; Desbiens, J.; Ritcey, A. M. *Langmuir* **2007**, *23* (5), 2843–2850.

62 Wang, B.; Li, B.; Dong, B.; Zhao, B.; Li, C. Y. *Macromolecules* **2010**, *43* (22), 9234–9238.

63 Cheng, L.; Song, J.; Yin, J.; Duan, H. *J. Phys. Chem. Lett.* **2011**, *2* (17), 2258–2262.

64 Cheng, L.; Liu, A.; Peng, S.; Duan, H. *ACS Nano* **2010**, *4* (10), 6098–6104.

65 Edwards, E. W.; Chanana, M.; Wang, D.; Möhwald, H. *Angew. Chem., Int. Ed.* **2008**, *47* (2), 320–323.

66 Boyer, C.; Whittaker, M. R.; Luzon, M.; Davis, T. P. *Macromolecules* **2009**, *42* (18), 6917–6926.

67 Gehan, H.; Mangeney, C.; Aubard, J.; Lévi, G.; Hohenau, A.; Krenn, J. R.; Lacaze, E.; Félidj, N. *J. Phys. Chem. Lett.* **2011**, *2* (8), 926–931.

68 Rezende, C. A.; Shan, J.; Lee, L.-T.; Zalczer, G.; Tenhu, H. *J. Phys. Chem. B* **2009**, *113* (29), 9786–9794.

69 Gibson, M. I.; Paripovic, D.; Klok, H.-A. *Adv. Mater.* **2010**, *22* (42), 4721–4725.

70 Yin, J.; Wu, T.; Song, J.; Zhang, Q.; Liu, S.; Xu, R.; Duan, H. *Chem. Mater.* **2011**, *23* (21), 4756–4764.